Ion transport through confined ion channels in the presence of immobile charges

Punyabrata Pradhan, Yariv Kafri, and Dov Levine
Physics Department, Technion-Israel Institute of Technology, Haifa, Israel

(Received 28 July 2009; revised manuscript received 21 February 2010; published 31 March 2010)

We study charge transport in an ionic solution in a confined nanoscale geometry in the presence of an externally applied electric field and immobile background charges. For a range of parameters, the ion current shows nonmonotonic behavior as a function of the external ion concentration. For small applied electric field, the ion transport can be understood from simple analytic arguments, which are supported by Monte Carlo simulations. The results qualitatively explain measurements of ion current seen in a recent experiment on ion transport through a DNA-threaded nanopore [D. J. Bonthuis *et al.*, Phys. Rev. Lett, **97**, 128104 (2006)].

DOI: 10.1103/PhysRevE.81.031928 PACS number(s): 87.16.Vy, 87.16.dp, 87.10.Mn

I. INTRODUCTION

Because of its central role in maintaining the homeostasis of cells, ion transport through channels across cell membranes is of great importance [1–4]. In a system with free ions, such as an aqueous solution, one might expect the ion current I to increase with increasing external ion concentration c when a constant electric field is applied. Surprisingly, in the presence of immobile charges fixed in the channel, the opposite may occur, with ion current decreasing with increasing c. For example, in the case of water-filled biological channels with strong ion binding sites, the ion conductance has been observed to reach a maximum and then decreases (or saturates) as c increases [5]; similar behavior is observed in DNA-threaded nanopores connecting two reservoirs [6].

An ion channel may be thought of as a thin hollow tube of length L where ions can enter or leave only through pores at the two ends. Because of the large difference in the dielectric constants of water ($\kappa_w \approx 80$) and the membrane containing the channel ($\kappa_m \approx 2$), introducing an uncompensated ion into the channel requires overcoming an energy barrier due to the ion's self-energy U_S [7]. The reason for this is that, because $\kappa_w \gg \kappa_m$, an ion's electric field lines are concentrated inside the channel over a length proportional to $l_1\sqrt{\kappa_w/\kappa_m}$, where l_1 is the shortest dimension of the channel [8]. The specific form that U_S takes depends on the nature of the channel. For a planar channel the electrostatic potential varies as $U(r) \sim \ln r$ for length scales $l_1\sqrt{\kappa_w/\kappa_m} > r > l_1$, while for a linear channel $U(r) \sim r$. For channels which are relatively short and narrow, the larger dimension of the channel $L \simeq l_1\sqrt{\kappa_w/\kappa_m} \gg l_1$; this implies that the self-energies scale as $\ln(L/l_1)/l_1$ and L/l_1^2 in planar ($l_1 \times L \times L$) and one-dimensional ($l_1 \times l_1 \times L$) geometries, respectively. For example, for a water-filled channel of dimensions $1 \times 1 \times 5$ nm^3, U_S is about 7 kT at $T = 300$ K where k is the Boltzmann constant [9].

Nonmonotonic behavior in charged channels was previously studied theoretically using a single vacancy model [10], under the assumption that the channel was strictly one-dimensional. A more recent study considered the ion current in a channel threaded with charged DNA, where the available space for ion motion was assumed to be effectively two-dimensional. In this case, the nonmonotonic behavior was attributed to the two-dimensional specifics of the channel and the self-energy of the ions, and to a boundary layer effect at the edges of the channel [6].

In this paper we present a many-particle statistical model of interacting ions, and argue that, in the presence of fixed background charges inside the channel, the large self-energy of an individual ion is sufficient to give rise to a nonmonotonic ion current I as a function of external ion concentration c. Our main result is that, irrespective of the effective channel dimension, there is a crossover temperature $T_* \simeq U_S/k$, below which the ion current may exhibit nonmonotonicity. However, above T_*, the ion current is a monotonically increasing function of c. Consequently, nonmonotonic behavior can be observed only when U_S is large enough for T_* to be above the freezing temperature of water. For example, when $U(r) \sim 1/r$, as in large three-dimensional cavities, T_* is much below the freezing temperature of water but when $U(r) \sim \ln r$, the $I(c)$ curve may have a minimum even at room temperature. In any case, for very high (or very low) density of background charges, I increases monotonically with c as is naively expected. This is summarized in Fig. 1.

The above results are the consequence of two main competing mechanisms for ion transport: (1) *Hopping current* I_h: At low temperature, the fixed background charges are screened by counterions, which thus reside in close proximity to the background charges—one may think of the counterions as sitting "on the sites" of the background charges.

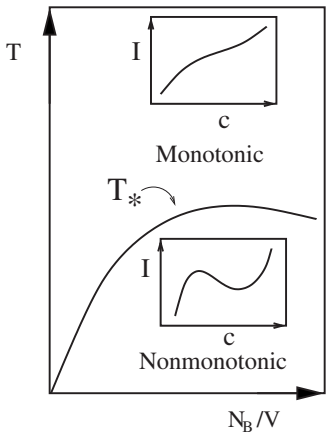

FIG. 1. Phase diagram of ion transport in a channel of confined geometry at temperature T and volume V with N_B immobile background charges inside the channel. The thick line denotes the crossover temperature T_*. The two insets are plots of ion current I versus external ion concentration c.

However, if one of the background charges is not screened (a "hole"), the screening counterion of an adjacent background charge can hop to it. I_h is approximately proportional to $\rho_h(\rho_0-\rho_h)$, where ρ_h is the density of holes, and ρ_0 is some constant. Since ρ_h decreases with increasing c, the ion current first increases, attains a maximum (at $\rho_h=\rho_0/2$) and then decreases. (2) *Bulk current* I_b: Ions that are not strongly attached to any counterions will move more or less freely inside the channel, and, biased by the electric field, will contribute to the total ion current. I_b is a monotonically increasing function of c. The total ion current I is sum of the hopping current I_h and the bulk current I_b, i.e., $I=I_h+I_b$.

It may be noted that the above intuitive picture for the hole current I_h has a quantitative description in terms of a simple model for driven diffusion, the *partially asymmetric simple exclusion process* (PASEP) [13]. The PASEP considers a one-dimensional lattice of sites, each of which may be either empty or occupied by a single particle. Particles may enter or leave the system at its ends, and a particle may hop to an adjacent site provided it is unoccupied. The parameters of the model are the rate of influx (α,γ) and outflux (β,δ) of particles at the left and right ends, respectively, and the hopping rates between sites: $q<1$ and 1, to the left and right, respectively (where the applied electric field may be thought of as the cause of asymmetry of the hopping rates). In the ion channel, a fixed charge screened by a counterion maps to an occupied site in the PASEP model, and an unscreened fixed charge maps to an unoccupied site in the PASEP.

The phase diagram of the PASEP model has been fully elucidated (see for example, [12,13]). If the incoming rates α and γ are taken to be proportional to the external ion concentration c, the behavior of current I_h can be immediately obtained using these results. It follows from [12] that $I_h\sim c$ for small c, and $I_h\sim 1/c$ for large c. At intermediate c, the current attains a maximum or a plateau. In the PASEP model, the various rates are taken to be constant, but, in reality, rates will depend on specific configurations of the system. Clearly the PASEP model cannot capture the appearance of the minimum in the $I(c)$ curve.

II. MODEL

To understand the full behavior of the ion current, we will consider a statistical mechanical model of interacting ions in an ion channel. We take the channel to be in contact with a reservoir of fixed chemical potential μ and temperature T. For simplicity, we will consider a discrete model, where the positions of ions lie on a lattice. For our model, we use the energy function of a system of N interacting ions of hardcore radius r_0, given by

$$H=\frac{1}{2}\sum_{i\neq j} q_i q_j U(r_{ij})+\frac{1}{2}U_0 N-\mu N, \tag{1}$$

where $q_i=\pm 1$ is the charge of ith ion, $U(r_{ij})$ is the interaction potential of ions i and j, whose separation is r_{ij}, N is the total number of ions and we denote $U_0\equiv U(r_{ij}=r_0)$; the self-energy of an ion is given by $U_S=U_0/2$. The definition of the Hamiltonian absorbs the chemical potential $\mu<0$, for simplicity assumed to be the same for both positive and negative ions, which is related to the fugacity $z=\exp(\mu/kT)$. The kinetic energy of the ions has been neglected, since ion motion in a fluid is overdamped. Additionally, we have assumed that the electrostatic potential $U(\vec{r})$ of a unit positive charge at position $\vec{r}$ inside the channel decays rapidly outside the channel.

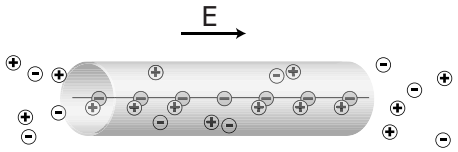

FIG. 2. Schematic representation of ion transport across a channel with a constant applied electric field E. The negative charges along the channel axis are immobile. All other ions are mobile, with their external concentration being c.

Note that inserting a bound neutral pair (one +, one − charge) costs an energy -2μ: because of cancellation there is no contribution from the first two terms in Eq. (1). The fugacity z controls the density of ions inside the channel. Ions can enter into the channel only through boundary sites at the channel's two open ends which are connected to the reservoir sites with ion concentration c. Assuming that the reservoir is modeled by a system of hard-core noninteracting particles of radius r_0, the ion concentration c of the reservoir is related to its fugacity by $c=v_0^{-1}z/(1+z)$ where $v_0=(4/3)\pi r_0^3$. For very small fugacity $z\ll 1$, the external ion concentration can be written as $c\approx z/v_0$.

When the externally applied electric field is not large, it is reasonable to assume that local thermal equilibrium is maintained. We thus include a constant external electric field $E\hat{x}$ along the channel axis. Using $\Sigma_{i\neq j}q_iq_j=[(\Sigma_i q_i)^2-\Sigma_i q_i^2]$, Eq. (1) may be rewritten

$$H_E=\frac{1}{2}\sum_{i\neq j} q_i q_j[U(r_{ij})-U_0]-E\sum_i q_i x_i - (N_+-N_--N_B)^2 kT\ln(z_b)-NkT\ln(z), \tag{2}$$

where we have explicitly indicated the N_B immobile negative background charges, and where the sum is over all pairs of ions except those where both are background charges. Here N_+ and N_- are the total number of positive and negative mobile ions respectively, $N=(N_++N_-)$, x_i the x coordinate of ith mobile ion, and $z_b\equiv\exp[-U_S/kT]$. For small z_b, charge fluctuations in a finite channel are small, and the channel remains almost charge-neutral $(N_+-N_--N_B)\simeq 0$ [11]. The process of ion transport across a channel is schematically presented in Fig. 2. In what follows, we present a small-fugacity (low external ion concentration) analysis of the model, whose results are then supported by numerical calculations.

III. RESULTS

Consider first the system at zero electric field; the charge distribution is then governed by the partition function

$$\mathcal{Z} = \sum \frac{1}{N_+! N_-!} e^{-\beta H_0},$$

where H_0 is the energy function of Eq. (2) with $E=0$, the sum is over all configurations (running over all values of N_+ and N_-, as well as positions of the charges), and $\beta \equiv 1/kT$. For small electric fields, i.e., either $qEr_0 \ll kT$ or $qEr_0 \ll q^2/\kappa_w r_0$ (interaction strength being much larger than the energy cost due to the electric field), the charge distribution will be essentially the same as for $E=0$; we will use this to calculate the ion current. In the experiment of [6], the electric field E is about 0.08 $kT/$Å per electronic charge (this corresponds to potential drop of 100 mV across an ion channel of length 5 nm), so our analysis should be applicable to the experiment. In what follows, we use numerics to explore also the regions where the small field assumption is violated, and show that the qualitative picture is still maintained.

We first analyze the model in the small fugacity limit $z \ll 1$, which corresponds to small external ion concentration ($c \simeq z/v_0$ as mentioned in Sec. II). Following this, we study the full model using Monte Carlo simulations.

A. Small fugacity expansion

Let us consider fugacities $z \sim z_b \ll 1$. In this limit, we may expand $\mathcal{Z}$ in powers of z and z_b. Collecting leading order terms, we obtain [14]

$$\mathcal{Z} \simeq z^{N_B} + N_B z^{N_B-1} z_b + \mathcal{O}(z^{N_B-2} z_b^4) + \mathcal{O}(V z^{N_B+1} z_b) + \mathcal{O}(V z^{N_B+2}), \tag{3}$$

where V is the channel volume measured in units of ionic volume. The terms on the right hand side have the following interpretations. z^{N_B}-all immobile charges are screened (no holes); $N_B z^{N_B-1} z_b$-a single unscreened immobile charge (one hole, which may be at any of the N_B positions); $\mathcal{O}(z^{N_B-2} z_b^4)$-two unscreened immobile charges (two holes); $\mathcal{O}(V z^{N_B+1} z_b)$-one excess positive or negative charge (apart from the screened backbone charges); $\mathcal{O}(V z^{N_B+2})$-one excess *bound* pair of positive and negative charges. The notation $\mathcal{O}(x)$ indicates that we do not explicitly write the combinatorial factor, that is, $\mathcal{O}(x) \propto x$. In the last two terms, the factor V accounts for the possible placements of the extra positive or negative charges. For $z_b \sim z \ll z_* \simeq \min\{V^{-1/2}, (z_b N_B/V)^{1/3}\}$, Eq. (3) can be well approximated by the first two terms alone, so the probability P_h that there is exactly one hole can be written as

$$P_h \approx \frac{N_B z^{N_B-1} z_b}{\mathcal{Z}} \simeq \frac{N_B z_b}{(N_B z_b + z)}. \tag{4}$$

In what follows, we will consider the behavior of the ion current in three fugacity regimes.

(i) *Regime I*: $z < z_b$

(ii) *Regime II*: $z_b < z \ll z_*$

(iii) *Regime III*: $z \gg z_*$

Regime I (small fugacity): If z is smaller than z_b, but not extremely small, the dominant contribution to Eq. (3) comes from one uncompensated immobile background charge (i.e., a hole). This means that current flows by sequential hopping of positive charges from one background charge to another: the hole moves from one end of the system to the other. The probability P_h of having one hole in the system depends weakly on z in this regime. Since $P_h \approx 1$ in this regime, the ion current is limited by the low external ion concentration. Therefore, for the current to flow, the hole must recombine with an ion from outside the channel; this occurs with a rate proportional to z/z_b, and therefore to c. This gives total ion current $I \approx I_h \sim z$ or $I \sim c$.

Regime II (intermediate fugacity): In this regime, the probability P_h of having one hole goes as $1/z$. Since for $z > z_b$ the recombination rate can be approximately taken as 1, the hole current is simply proportional to the hole density, so that

$$I_h \approx \sigma \times \frac{z_b}{(N_B z_b + z)}, \tag{5}$$

where σ is a constant related to the jump rate of a hole from site to site along the backbone of immobile charges. Since such motion may be thought of as hopping between potential wells, σ may in principle be calculated from Kramers' theory in the presence of a driving force (the electric field). In this regime, where the charge concentration is low, σ is independent of z to leading order.

Regime III is the large fugacity limit $1 \gg z \gg z_*$, where extra charges enter the system, although the immobile background charges are already fully compensated. In this regime the ion current is expected to increase with increasing fugacity. Since neutral pairs of charges will enter the channel more easily than uncompensated charges, the number of charges inside the channel should increase as $z^2 \propto c^2$. Thus, the ion current is expected to behave as $I \propto c^2$.

In sum, as a function of increasing external ion concentration c, we have the following picture: The ion current rises linearly as $I \sim c$ in Region I, falls inversely with c as $1/c$ in Region II, and rises again approximately as $I \sim c^2$ in Region III. Thus, it is the passage from Regime I to II that determines the nonmonotonic behavior. One should note that the minimum in the $I(c)$ curve occurs approximately at the external ion concentration $c \sim z_*/v_0$. We note however, that in some cases, Regime II may be unobtainable—this happens when $z_* < z_b$. In this case, Regime I crosses smoothly over to Regime III, and the ion current increases monotonically with c over its entire range. In other words, Regime II is present only if $T < T_*$, where $T_* = 2U_S/k \ln(V/N_B)$. This can be seen by comparing the two terms, second and fifth, in Eq. (3) in the fugacity region $z \sim z_b$ where nonmonotonic behavior in $I(c)$ may appear.

Note that T_* increases with the number of bound charges N_B. This increase in T_* can be understood from a simple physical picture. When $N_B \ll V$, the bulk density of excess unbound ions are far greater than the hole density inside the channel, due to the large entropic volume factor V in Eq. (3). Thus the bulk current always dominates over the hole current. Since the bulk current is a monotonic function of c, there will be no minimum in the $I(c)$ curve. On the other hand, for larger $N_B < V$, the density of holes increases in the channel, and with it the hole current which dominates now.

Since the hole current is nonmonotonic in c, a minimum appears in the $I(c)$ curve.

The above picture breaks down when the density of immobile background charges, and therefore the density of screening counterions, is so high that an ion is no longer bound to any specific background charge and can move freely (without hopping) from one background charge to another. This occurs when the typical distance between background charges is smaller than the screening length. Essentially in this case, the hopping barrier between neighboring background charges decreases as the background charge density increases. Under such conditions of very high immobile background charge density, we expect the ion current to increase monotonically with external ion concentration.

B. Numerical results

To support these simple arguments, we have performed Monte Carlo simulations. For computational convenience, ions are only allowed to move in discrete steps on a square lattice, with each site able to accommodate at most one ion. Ions can enter and leave the system only from two opposite surfaces, representing the pores of the channel. We denote by ΔH_E and ΔH_0 the energy difference between configurations after and before a possible Monte Carlo move, where H_E and H_0 are, respectively, the Hamiltonians in Eq. (2) with and without the electric field. The simulation is carried out by performing the following two steps.

(1) *Creation/destruction of charges*: A boundary site is chosen randomly and, if it is empty, a positive (negative) charge is created with probability $min\{\frac{1}{2}, \frac{1}{2}e^{-\Delta H_0/kT}\}$. If the site is occupied, the charge is destroyed with probability $min\{1, e^{-\Delta H_0/kT}\}$.

(2) *Movement of charges in the bulk*: A site in the interior of the lattice is chosen randomly and, if occupied, its charge is moved to a randomly chosen unoccupied neighboring site (which is also in the interior of the lattice) with probability $min\{\frac{1}{4}, \frac{1}{4}e^{-\Delta H_E/kT}\}$.

In the Monte Carlo simulations, these two steps are performed repeatedly and every site is updated with rate one per Monte Carlo time step. Note that in step (1), an update attempt is accepted/rejected on the basis of calculating ΔH_0 (not ΔH_E) to ensure equal densities at the two boundaries of the system. For $E=0$, the system eventually comes to equilibrium, while for $E \neq 0$, the system settles into a nonequilibrium steady state with a net ion current across the channel in the x direction.

Motivated by the experiment of Ref. [6] which is effectively two-dimensional, we performed a simulation on an $L \times L$ lattice using the above protocol, with the interaction potential taken to be $U(r)=(2e^2/\kappa_w r_0)\ln(L/r)$, where e is the electron charge, and $r_0 \simeq 0.35$ nm [6]. An immobile linear array of equally spaced unit negative charges is placed on a line parallel to the x axis in the middle of the channel, at $y=L/2$, to mimic the presence of charged ss-DNA in the experiment. One should note that when L is large and $N_B=0$, Eq. (2) is the two-dimensional (2D) Coulomb gas Hamiltonian [15].

In Fig. 3 we plot the total ion current versus external ion concentration for different temperatures. As expected from

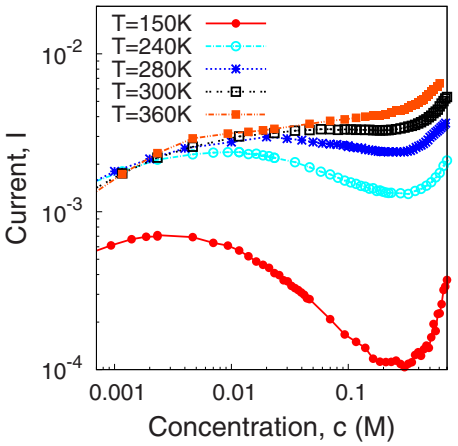

FIG. 3. (Color online) Ion current I (in arbitrary units) vs external ion concentration c (in Moles) is plotted for different temperatures. Here $L=30\times d_{K^+}$ where the diameter d_{K^+} of a K^+ ion is 0.26 nm, $E=5.4$ mV/nm along x axis, $N_B=6$ negative immobile background charges.

the arguments presented above, the numerical results are qualitatively different in two different temperature regimes. For $T<T_* \approx 300$ K, the ion current I first increases with c for small c, then reaches a maximum and subsequently decreases [16]. Increasing c further, I reaches a minimum and then starts increasing with c. In our simulation, the $I(c)$ curve for $T=280$ K has a shallow minimum which occurs slightly below $c=0.3$ M, in reasonable agreement with the experiment [6] where the minimum occurs near $c=0.5$ M. The maximum in the $I(c)$ curve in the simulation occurs at $c \approx 0.03$ M. This regime was not probed in the experiment of [6]. For $T>T_*$ the ion current I is a monotonically increasing function of external ion concentration c. The numerical value of $T_* \simeq 300$ K is somewhat smaller than $T_* = 2U_S/[k \ln(V/N_B)]=816$ K, the value predicted from the small fugacity expansion. Such order of magnitude agreement is about all that could be expected from such a simple argument.

In Fig. 4, we plot numerical results for the ion current I, the probability P_h that the system has exactly one hole, and the average total number of ions n per site as a function of

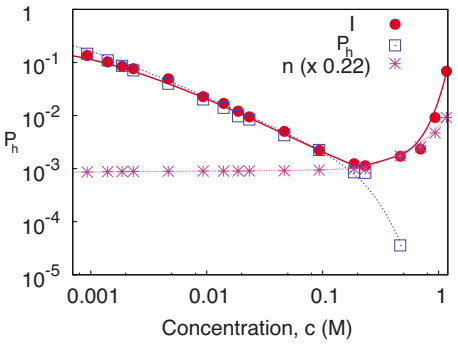

FIG. 4. (Color online) Ion current I (in arbitrary units), probability P_h of exactly one hole and average total number of ions per site n, plotted versus external ion concentration c (in Moles). Here $E=1.1$ mV/nm, $T=150$ K, $L=30\times d_K$, $z_b=1.23\times 10^{-6}$ and $N_B=6$. n has been scaled by a factor 0.22 so that it fits in the figure.

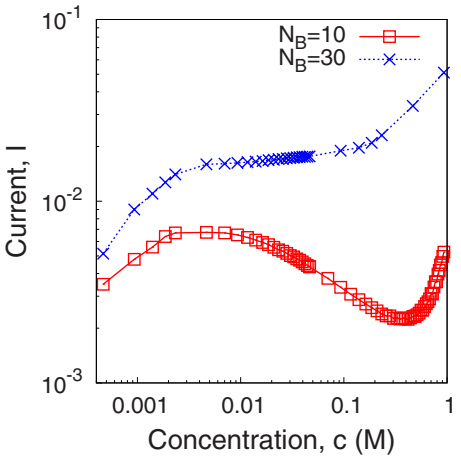

FIG. 5. (Color online) Ion current I (in arbitrary units) vs external ion concentration c (in Moles) for two different values of N_B. Here $T=150$ K, $E=25.0$ mV/nm along the x axis, and $L=30\times d_{K^+}$, where the diameter d_{K^+} of a K^+ ion is 0.26 nm. For a linear array of background charges in the middle (along $y=L/2$) with large $N_B=30$, even at a very low temperature $T=150$ K, there is no minimum in the ion current vs external ion concentration curve.

the external ion concentration where both P_h and n are scaled suitably to relate to I for $T<T_*$. As can be seen at low external ion concentrations ($c\leq 0.2$), single hole hopping is responsible for the ion current. For larger external ion concentrations, the number of free bulk ions increases, and the ion current, almost entirely due to flowing ions in the bulk, rises. For large self-energies, as explained in Sec. III A, the number of unbound charges inside the system increases as c^2 for $z_*<cv_0\ll 1$. This is also observed in the simulations which can be seen in Fig. 4 showing a concomitant rise in ion current. In Fig. 4 the ion current I, scaled probability P_h of exactly one hole and scaled total number of ions/site n is plotted versus external ion concentration c with an electric field $E=1.1$ mV/nm, temperature $T=150$ K, $L=30\times d_K$ where $d_K=0.26$ nm is the diameter of a K^+ ion, $z_b=1.23\times 10^{-6}$ and $N_B=6$ negative immobile background charges. Note that the analytic expressions for the probability of one-hole configuration and the hole current, as given in Eqs. (4) and (5), are valid in the small electric field limit when $qEr_0\ll kT$ or $qEr_0\ll q^2/\kappa_w r_0$. At very low temperature, the condition $qEr_0\ll kT$ may be violated. However, the condition $qEr_0\ll q^2/\kappa_w r_0$, which is independent of any temperature, is well satisfied where $(qEr_0)\times(\kappa_w r_0/q^2)\simeq 0.07$ with $E=20$ mV/nm and q the electronic charge [17].

In Fig. 5, we have plotted the ion current as a function of external ion concentration for $T=150$ K for two different values of N_B, where the linear immobile background charge array is kept in the middle of a 30×30 lattice. As discussed at the end of the previous section, very large N_B leads to a decrease in the hopping barrier between the immobile charges which flattens out the minimum in the $I(c)$ curve. We see that, for very large value of N_B, i.e., when the immobile charges are located very close to each other, there is no observed minimum in the $I(c)$ curve even at the very low (and experimentally inaccessible) temperature $T=150$ K.

Finally, it is worth noting the influence of the effective dimension of the system, which manifests itself in the functional form of the Coulomb interaction. In Monte Carlo simulations of the same geometry (a 30×30 lattice with a linear array of $N_B=6$ negative immobile charges in the middle), but employing the faster decaying Coulomb interaction $U(r)=1/r$ appropriate to three dimensions, we found that a minimum in the $I(c)$ plot can in principle occur. However, this occurs only at extremely low temperatures: $T\sim 36$ K which is clearly experimentally irrelevant. In Fig. 6, $I(c)$ is plotted for different temperatures with an electric field $E=5.4$ mV/nm applied in the x direction.

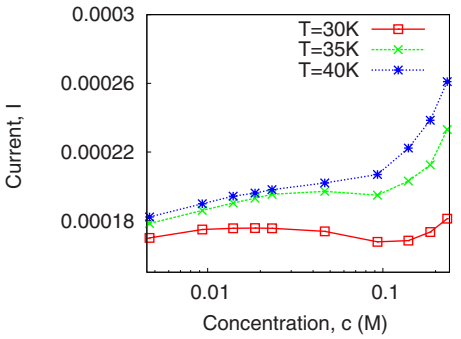

FIG. 6. (Color online) Coulomb interaction $U(r)\sim 1/r$: Ion current I (in arbitrary units) vs external ion concentration c (in Moles) plotted for different temperatures. Here $E=5.4$ mV/nm along the x axis, $N_B=6$, and $L=30\times d_{K^+}$, where the diameter d_{K^+} of a K^+ ion is 0.26 nm.

This demonstrates that the nonmonotonic behavior of $I(c)$ does not depend in an essential way on the existence of a Donnan potential as suggested in [6]. In particular, the essential ingredient for the nonmonotonicity is the large self-energy of an ion in the channel, resulting from the large disparity between the dielectric constants and the small dimensions of the channel, and enhanced by the long-range nature of the Coulomb interaction in two dimensions. Under other conditions, we would not expect T_* to be large enough for the effect to be observed.

Finally, in addition to electrostatic interactions, one might inquire as to the importance of hydrodynamic interactions. It is easy to see that hydrodynamic interactions are important only for systems which are much larger than some characteristic scale R_*. The length scale R_* may be estimated by comparing the electrostatic and the hydrodynamic forces between two ions separated by a distance r. In SI units, the electrostatic interaction (in three dimensions) is $f_E=\frac{e^2}{4\pi\epsilon_0\kappa_w r^2}$ while the hydrodynamic force is $f_H=\gamma u_d r_0/r$, γ is the viscous drag coefficient, ϵ_0 is the dielectric constant of the vacuum, r_0 is the radius of the ion, e is the charge of the ion and u_d is the ion drift velocity. Taking $u_d=(eE/\gamma)$, where E is the electric field acting on the ions in the channel, we obtain $R_*=e/(4\pi\epsilon_0\kappa_w r_0 E)$. For the experimental conditions of [6], $R_*\approx 10$ nm which is larger than the channel scale (the same result holds in two dimensions). In this paper our interest has been in this regime, consequently we have ignored hydrodynamic interactions.

IV. SUMMARY

We have studied charge transport across a nanoscale ion channel in an ionic solution, in the presence of an external

electric field and immobile background charges in the channel. For a range of parameters, the ion current shows nonmonotonic behavior as a function of the external ion concentration in the solution. When the applied electric field is small, the ion transport can be understood from simple analytic arguments, which are supported by Monte Carlo simulations. We argue that for any finite self-energy of the mobile ions in the channel, nonmonotonic behavior in the current-concentration curve always results at sufficiently low temperatures. Our results compare well with the recent experiments presented in [6].

ACKNOWLEDGMENTS

D.L. and Y.K. acknowledge support from the Israel Science Foundation under Grant Nos. 1574/08 and 1183/06. P.P. acknowledges support from the Russell Berrie Nanotechnology Institute at the Technion.

[1] B. Hille, *Ion Channels of Excitable Membranes* (Sinauer Associates, Sunderland, MA, 2001).
[2] B. Roux, T. Allen, S. Berneche, and W. Im, Q. Rev. Biophys. **37**, 15 (2004).
[3] D. A. Doyle *et al.*, Science **280**, 69 (1998).
[4] A. Meller, J. Phys.: Condens. Matter **15**, R581 (2003).
[5] S. B. Hladky and D. A. Haydon, Biochim. Biophys. Acta **274**, 294 (1972); G. Eisenman, R. Latorre, and C. Miller, Biophys. J. **50**, 1025 (1986); A. Finkelstein and O. S. Andersen, J. Membr. Biol. **59**, 155 (1981).
[6] D. Jan Bonthuis, J. Zhang, B. Hornblower, J. Mathe, B. I. Shklovskii, and A. Meller, Phys. Rev. Lett. **97**, 128104 (2006).
[7] V. A. Parsegian, Nature (London) **221**, 844 (1969).
[8] S. Teber, J. Stat. Mech.: Theory Exp. (2005) P07001.
[9] J. Zhang, A. Kamenev, and B. I. Shklovskii, Phys. Rev. Lett. **95**, 148101 (2005).
[10] M. F. Schumaker and R. MacKinnon, Biophys. J. **58**, 975 (1990).
[11] Y. Rabin and M. Tanaka, Phys. Rev. Lett. **94**, 148103 (2005).
[12] M. Uchiyama, T. Sasamoto, and M. Wadati, J. Phys. A **37**, 4985 (2004).
[13] R. A. Blythe and M. R. Evans, J. Phys. A **40**, R333 (2007); R. A. Blythe, M. R. Evans, A. F. Colaiori, and F. H. L. Essler, *ibid.* **33**, 2313 (2000); T. Sasamoto, *ibid.* **32**, 7109 (1999).
[14] We note that in Eq. (2) the energy cost for neutral pairs of mobile ions grows with the number of ions, whereas the energy cost for holes grows with square of the number of holes. For this reason the single hole term is obtained from the weight factor of the charge-neutral configuration z^{N_B} multiplied by z_b/z (z_b/z is associated with creation of only a single hole.), whereas the weight for a two-hole configuration is obtained from z^{N_B} multiplied by z_b^4/z^2, not $(z_b/z)^2$.
[15] P. Minnhagen, Rev. Mod. Phys. **59**, 1001 (1987).
[16] J. M. Kosterlitz and D. J. Thouless, J. Phys. C **5**, L124 (1972).
[17] Taking $T=300$ K, $E=20$ mV/nm, q the electronic charge, $r_0=2.6$ Å and $\kappa_w=80$, we get $qEr_0 \simeq 0.2$ kT and $q^2/\kappa_w r_0 \simeq 2.7$ kT.